Successful evaluation for space applications of the 2048x1080 DMD

Frederic Zamkotsian[1], Patrick Lanzoni[1], Emmanuel Grassi[1], Rudy Barette[1], Christophe Fabron[1], Kyrre Tangen[2], Luca Valenziano[3], Laurent Marchand[4], Ludovic Duvet[4]

[1] Laboratoire d'Astrophysique de Marseille, CNRS, 38 rue Frederic Joliot Curie, 13388 Marseille Cedex 13, France
[2] Visitech, Kjellstadveien 5, Lier, P.O.Box 616, N-3003 Drammen, Norway
[3] INAF/IASF Bologna, via P. Gobetti 101, I-40129 Bologna, Italy
[4] European Space Agency, Keplerlaan 1, 2200 AG, Noordwijk, The Netherlands

E-mail address: frederic.zamkotsian@oamp.fr

ABSTRACT

Next-generation infrared multi-object spectrographs (MOS) for ground-based and space telescopes could be based on MOEMS programmable slit masks. This astronomical technique is used extensively to investigate the formation and evolution of galaxies.
ESA has engaged a study for a technical assessment of using a DMD from Texas Instruments for space applications. The DMD features 2048 x 1080 mirrors on a 13.68µm pitch, where each mirror can be independently switched between an ON (+12°) position and an OFF (-12°) position. For MOS applications in space, the device should work in vacuum, at low temperature, and each MOS exposure would last for typically 1500s with micromirrors held in a static state (either ON or OFF). A specific thermal/vacuum test chamber has been developed for test conditions down to -40°C at 10^{-5} mbar vacuum. Imaging capability for resolving each micromirror has also been developed for determining degradation in any single mirror. Our first tests reveal that the DMD remains fully operational at -40°C and in vacuum. A 1038 hours life test in space conditions, Total Ionizing Dose radiation, thermal cycling and vibrations/shocks have also been successfully completed. These results do not reveal any concerns regarding the ability of the DMD to meet environmental space requirements. Detailed analysis of micromirror throughputs has also been studied for a whole set of tests, and shows a rather low variation and no impact of the space environment.
We have also developed a bench for MOS demonstration using MOEMS devices. DMD chip has been successfully tested revealing good contrast values as well as good functionality for applying any mask pattern, demonstrating its full ability for space instrumentation, especially in multi-object spectroscopy applications.

Keywords: micromirror array, space evaluation, multi-object spectrograph, EUCLID mission, MOEMS.

1. INTRODUCTION

Next-generation infrared astronomical instrumentation for ground-based and space telescopes could be based on MOEMS programmable slit masks for multi-object spectroscopy (MOS). This astronomical technique is used extensively to investigate the formation and evolution of galaxies. The so-called EUCLID mission from the European Space Agency (ESA) will study the dark universe by characterizing a very high number of galaxies in shape and in spectrum. In order to optimize the Signal-to-Noise Ratio (SNR) value, the high precision spectra measurements could be obtained via multi-object spectroscopy (MOS). Multi-object spectroscopy (MOS) with multi-slits is the best approach to eliminate the problem of spectral confusion, to optimize the quality and the SNR of the spectra, to reach fainter limiting fluxes and to maximize the scientific return both in cosmology and in legacy science. Major telescopes around the world are equipped with Multi-Object Spectrographs (MOS) in order to simultaneously record several hundred spectra in a single observation run. Next generation MOS for space like the Near Infrared Multi-Object Spectrograph (NIRSpec) for the James Webb Space Telescope (JWST) require a programmable multi-slit mask. Conventional masks or complex fiber-optics-based mechanisms are not attractive for space. The programmable multi-slit mask requires remote control of the multi-slit configuration in real time.

A promising possible solution is the use of MOEMS devices such as micromirror arrays (MMA) [1,2,3] or micro-shutter arrays (MSA).[4] MMAs are designed for generating reflecting slits, while MSAs generate transmissive slits. MSA has been selected to be the multi-slit device for NIRSpec and is under development at NASA's Goddard Space Flight

Emerging Digital Micromirror Device Based Systems and Applications III, edited by Michael R. Douglass, Patrick I. Oden, Proc. of SPIE Vol. 7932, 79320A · © 2011 SPIE
CCC code: 0277-786X/11/$18 · doi: 10.1117/12.876872

Center. They use a combination of magnetic effect for shutter actuation, and electrostatic effect for shutter latching in the open position. In Europe, an effort is currently under way to develop single-crystalline silicon micromirror arrays for future generation infrared multi-object spectroscopy.[5] By placing the programmable slit mask in the focal plane of the telescope, the light from selected objects is directed toward the spectrograph, while the light from other objects and from the sky background is blocked. For example, a MOEMS-based MOS concept where the programmable slit mask is a MMA is shown in the left-hand side of Fig. 1. In action, the micro-mirrors in the ON position direct the light toward the spectrograph and appear bright, while the micro-mirrors in the OFF position are dark.

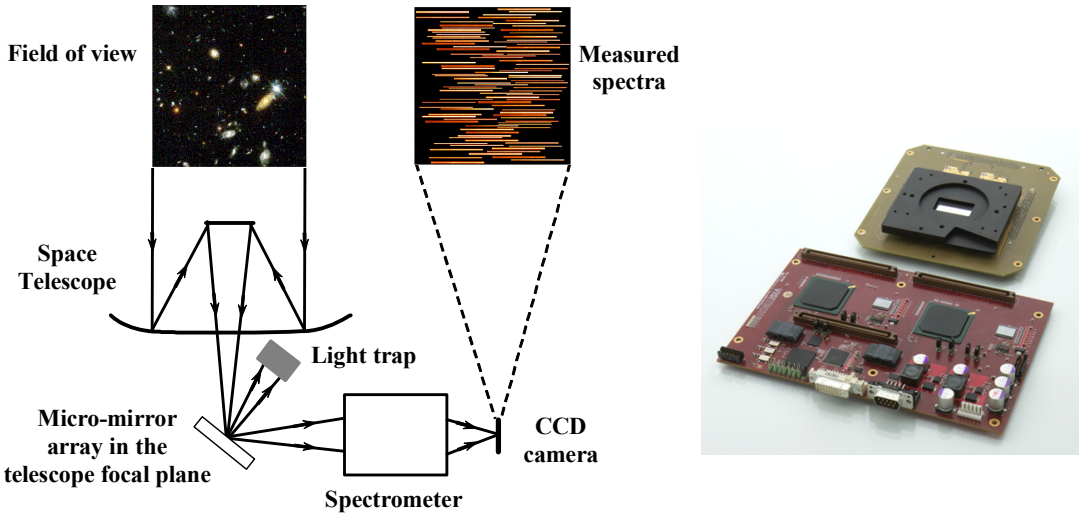

Fig. 1: Principle of a Multi-Object Spectrograph with a Micro-Mirror Array.
DMD chip from Texas Instruments (2048 x 1080 micromirrors) and its electronics.

In the timescale of the EUCLID mission, a specialized programmable multi-slit mask cannot be developed. This component has to be commercially available. To get more than 2 millions independent micromirrors, the selected component for an EUCLID pre-study is a DMD chip from Texas Instruments that features 2048 x 1080 mirrors and a 13.68µm pixel pitch (right-hand side of Fig. 1). Typical operational parameters are room temperature, atmospheric pressure and mirrors switching thousands of times in a second, while for EUCLID, the device should work in vacuum, at low temperature, and each MOS exposure lasts between 400s and 1500s, with mirrors held in one state (either ON or OFF) during the exposure.

Visitech is an engineering company experienced in developing DMD solutions for industrial customers. The Laboratoire d'Astrophysique de Marseille (LAM) has, over several years, developed different tools for modeling and characterization of MOEMS-based slit masks, especially during the design studies on JWST-NIRSpec. [6, 7] ESA has engaged with Visitech and LAM in a technical assessment of a DMD chip for space application. A specific thermal / vacuum test chamber has been developed for test conditions down to -40°C at 10^{-5} mbar vacuum. Imaging capability for resolving each micro-mirror has also been developed for determining any single mirror failure. Dedicated electronics and software allows us to hold any pattern on the DMD for duration of up to 1500s.

We present the summary of this ESA study, the electronic test vehicle as well as the cold temperature test set-up we have developed. Then, results of tests in vacuum at low temperature, including low temperature stress test, low temperature nominal test, thermal cycling, and life test are presented. Results after radiation (TID and proton), and vibration and shock are also shown. Detailed analysis of micromirror throughput is also developed. Finally MOS-like tests have been done.

2. THE ELECTRONIC TEST VEHICLE

The DMD driver electronics consists of a formatter board and a DMD board. The general architecture of the system is described elsewhere. [8, 9] There is a notable difference that separates this system from other DMD board designs; the control signals of the reset drivers are fed through an FPGA. This enables splitting the DMD into five zones with each zone being driven with a different pattern and refresh rate. This functionality reduces the number of test vehicles and test duration because several conditions can be tested in parallel on the same DMD. The electronic test vehicles were designed by Visitech for extreme test conditions using essentially commercial off the shelf components.

3. COLD TEMPERATURE TEST EQUIPMENT AND PROCEDURE

The Laboratoire d'Astrophysique de Marseille has over the last few years developed an expertise in the characterization of micro-optical components. [7,10,11] This expertise in small-scale surface deformation characterization of micro-optical components as well as operational testing of MOEMS components has been used for developing a dedicated cold temperature test set-up for DMD measurements in EUCLID operating conditions.

3.1 Cryostat & optical bench

For environmental testing (vacuum and low temperature), a cryostat has been developed at LAM. The bench (Fig. 2) is used as a photometric bench. In order to get enough resolution on each micromirror, the FOV images approximately 200x200 micromirrors onto a 1k x 1k camera. To inspect the complete DMD, a stitching procedure is carried out, by means of motorized stages. For the sake of test accuracy and efficiency, the characterization set-up is automated as much as possible. Three computers are used for managing the tests. The thermal chamber enables tests in a vacuum environment with temperature adjustment in the range of -60°C to +20°C. Temperature change is obtained through a liquid cooler. The chamber is made of a stainless steel cross. Each side is devoted to a specific task. The first side includes a window in order to view the DMD sample; the second side holds the feed-through connectors for driving the DMD board; the third side permits all sensing wires (for temperature sensors) to pass into the chamber. Finally, the fourth side receives the pipes from the liquid cooler device. The cryostat is monitored with temperature sensors and vacuum sensors driven by a computer (*cryostat computer* in Fig. 2). Illumination of the DMD array is made by a collimated beam. Optical imaging is made by two doublets (200mm – 400mm) mounted on rail. The system is diffraction limited on the detector, leading to an optimized photometric measurement. The device is divided into **50 zones**. The FOV to be imaged by the CCD camera covers one zone, equivalent to **205 x 216 micromirrors** (44280 micromirrors). The plate scale on the 1k x 1k camera is exactly 4.07 x 4.07 detector pixels / micromirror. For complete DMD testing, the stitching procedure is done by means of motorized stages in three directions (XYZ) moving the whole imaging optical train, with a travelling range of 100mm and a resolution of 0.1µm. The optical test equipment (stages + camera) are monitored by a computer (*test computer* in Fig. 2). All software is developed in Matlab.

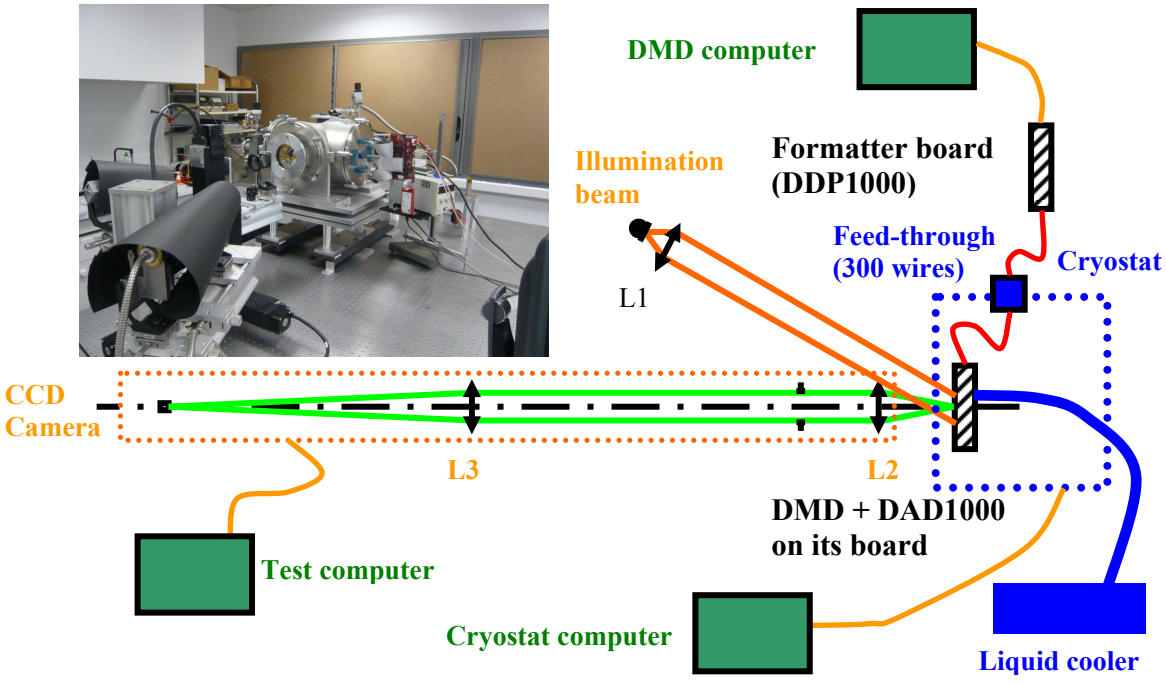

Fig. 2: Cold temperature test set-up

The DMD board is mounted on the thermal interface through a point-plane-plane mounting scheme in order to avoid any additional stress on the board when the temperature is changing. The thermal link between the thermal interface and the DMD board as well as the DMD itself is done through copper wires connected to the DMD board, the DMD heat

sink and the front mounting surface of the DMD device (Fig. 5, left-hand image). The DMD board is linked by 300 wires through the chamber to the formatter board. Specialized feed-throughs for such high number of wires has been realized, tested, and have been mounted on our chamber. All materials used in the chamber are vacuum compatible, except the wires leading to the DMD board and some parts on the DMD board. After DMD board integration, the thermal screen with Multi-Layer Insulator (MLI) cover is mounted around the device, and the optical window is closed on the chamber. We have decided to align and fix the optical input and output beams as a very precise and reliable reference. Then all optical alignments are performed on the chamber, using the tip-tilt and rotation mounting under the cryo chamber. When the DMD chip and the detector are in parallel planes, the stitching of the images could be done much easier with the motorized stages moving the optical train. A focused image across the whole device is maintained without the need for Z stage adjustment during stitching with the X and Y stages. By this way, the optical input and output beams stay fixed with respect to the DMD.

3.2 Device driving

Hardware and software were developed by Visitech and LAM for driving the DMD boards. The hardware is controlled by a RS-232 serial link and a DVI port is used for loading an image onto the DMD. The software is developed in Matlab for driving the DMD chip by a computer (*DMD computer* in Fig. 2).

In addition to the extreme conditions of a EUCLID environment, this DMD-based instrument also has a very non-typical DMD operation: during data capture, each DMD micromirror will be held in one position for 1500 seconds before changing state. This is quite a challenge to accomplish with a DDP1000 based chip set and testing is required in static ON and static OFF modes in addition to normal display-type operation. Normal display-type operation is used as a base line in analyzing test results. Schedule of the ESA activity did not allow for testing static and normal display-type modes on separate devices. To meet all requirements, each DMD has been divided into 5 horizontal rows and each row can be driven in normal display-type mode or static modes (Fig. 3). This allows for testing of all modes on a single DMD at the same time. 4/5 of the DMD operates in a static ON or OFF mode (arbitrary pattern) and 1/5 of the DMD operates in display-type mode where the pattern is updated at 1Hz rate. This results in a display-type zone of roughly 400 000 micromirrors and static zones of 4 times this size, which is an ample amount for statistical analysis of the test results.

The two major patterns, pattern 1 and pattern 2, are designed as “positive” and “negative” to each other (Fig. 3). Each pattern row is divided in 10 zones for a total of 50 zones, and each zone is imaged on the CCD camera. Each zone includes specific patterns identical from zone to zone and numbers at the edge of each zone are set for easy processing and archiving (central picture of Fig. 3). The individual patterns show lines with different width and orientation, chessboard features and MOS-like patterns. In addition to pattern 1 and pattern 2, all ON and all OFF mirrors will also be displayed and measured at each measurement step. Background will be measured and subtracted from the images.

Each micromirror is imaged on the CCD camera on about 4x4 detector pixels, which is enough for monitoring and detection of failures (if any) during the tests. A zoom on the area simulating a MOS-like pattern, with multi-slits is shown in right-hand side of Fig. 3. Any slit location and shape can be generated. It has to be noticed that the OFF mirrors cannot be imaged on the detector due to the high contrast performance of DMD. Then, the contrast cannot be measured in this test. An evaluation of the contrast will be done during the MOS-like tests, using a high dynamic range camera.

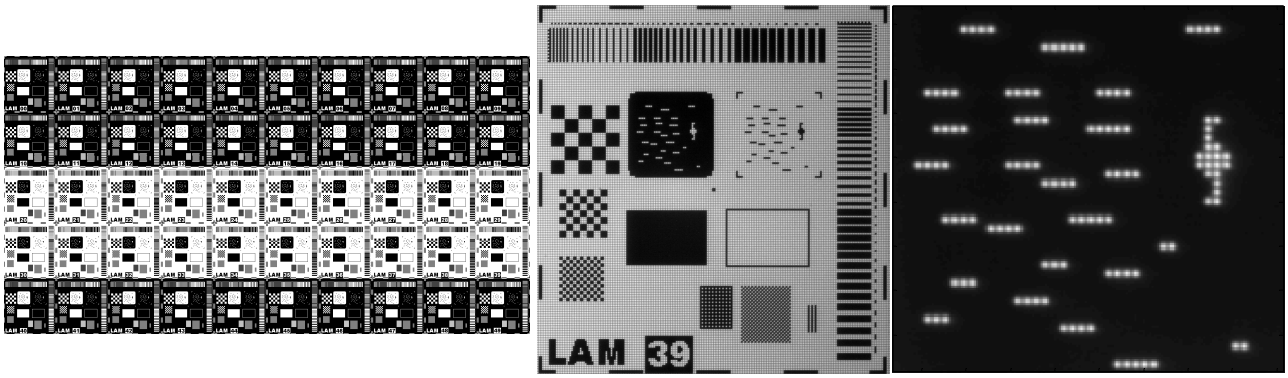

Fig. 3: LAM designed pattern (pattern 1); Image of a zone taken with the characterization set-up CCD camera and close-up view on a MOS-like pattern

3.3 Analysis procedure

A data pipeline for data reduction has been developed using Matlab software. Photometric measurements are done before, during and after each test, and compared to the reference measurements (taken before the test, at room temperature). Any degradation in performance of a mirror will be revealed. Differences between mirrors as well as tests on different patterns applied on the same device (patterns in space domain and time domain) will be analyzed. The analysis procedure comprises background subtraction, pattern recentering, mirror envelop detection, mirror photometric measurement, comparison with the nominal mirror photometric measurement; local variations of the illumination beam are taken into account. We have adopted three mirror degradation definitions: - the **blocked mirror** when the mirror is non-responsive (e.g. "stuck"), - the **lossy mirror** when the optical throughput is decreased by more than 20%, and – the **weak mirror** when the optical throughput is decreased between 10% and 20%. Typical images of these types of mirrors are shown in Fig. 4 (central mirror in each image). Blocked mirrors show a lack of light on the micro-mirror area, while for lossy and weak mirrors, a decrease in the throughput is observed. For automatically detecting these mirrors, we have defined two parameters: **micro-mirror average throughput calculation** and **centroid calculation**. The micro-mirror average throughput is the flux integrated in the area of each micro-mirror. The centroid is calculated within the area of the micro-mirror and located on the map, as displayed in Fig. 4. For blocked mirrors, there is a major shift while for lossy mirrors, the shift is small. There is nearly no shift for weak mirrors.

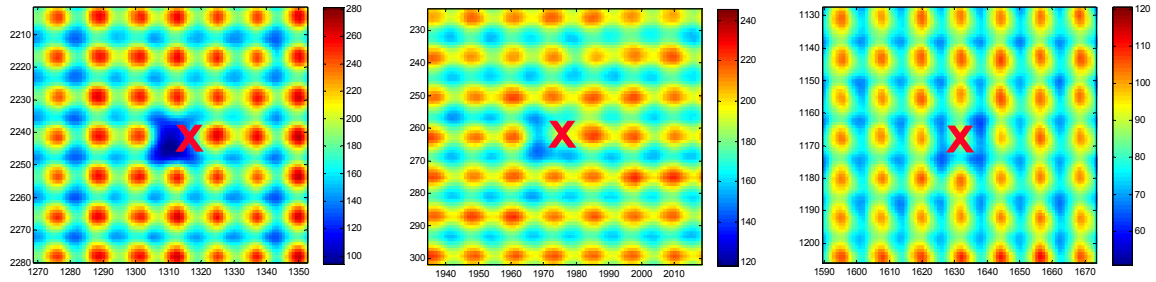

Figure 4: Three types of mirrors with failure: blocked, lossy and weak; centroid locations are marked with an "x".

We have developed software for an automatic analysis of all data recorded during our measurements. All failure types are searched and detected. Results are displayed into maps and graphs. In some cases, the mirrors could appear with an extra-brightness (extra-throughput in the range + 10% to 20%). After the first analysis process, a second level of analysis is done: we name it as a cleaning process, for removing false failure detections. The false failure detections are due mainly to dust particles present on the camera or the DMD window. Dust on the camera is revealed by failure detection located in the same area for each zone, while dust on the DMD window will appear in the same place on the DMD from measurement to measurement. Some mirrors flagged as affected could be false detection due to very small dust particles, but this effect could affect only marginally the weak mirrors. The final results are then given in three graphs (example: Fig. 6) showing the number and the locations of failed mirrors (blocked, lossy and weak). All fifty zones from the DMD are shown in a matrix pattern (zone 00 to zone 49), and the number of affected mirrors is assigned to each zone. Comparison of measurements before and after testing shows the evolution of the failure rate.

4. COLD TEMPERATURE TEST

Four sets of cold temperature tests have been completed: cold temperature step stress test, nominal cold temperature test, thermal cycling and life test. Pictures of the device mounted in the chamber during life test in LAM's cold chamber are shown in Fig. 5.

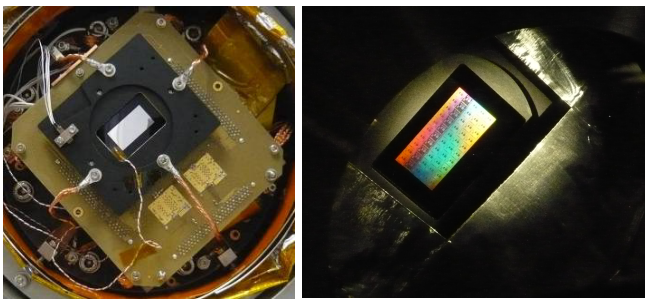

Fig. 5: Pictures of the device during life test.

4.1 Cold temperature step stress test and nominal cold temperature test

The cold temperature step stress test has been done from room temperature down to -60°C. **This test shows that permanent failure, i. e. stuck mirrors, is appearing on some mirrors when the device is taken down to -55°C.** The failure rate increases at -60°C.

Based on these results, the nominal temperature condition for EUCLID was set to -40°C. In order to confirm that this is an acceptable nominal operating condition for the device, a single DMD was tested. The DMD was mounted in the cold temperature chamber and tested three times at this temperature. For minimizing stress on the device when cooling down, a fast (-40°C / hour) and homogeneous cooling was provided. Using the definitions of blocked, lossy and weak mirrors, we have analyzed all (over 2 million) mirrors from the DMD for each measurement. No blocked mirror was revealed while only 12 mirrors are defined as lossy, and between 3 to 7 as weak mirrors. According to the screening procedure of TI where all mirrors are considered to be either working or not working, this measurement shows intermediate states where lossy and weak mirrors are observed; lossy mirrors stay lossy during the whole test, and weak mirrors may change in status from test to test; all other mirrors show their full performances. This effect is possibly due to local non-uniformity at individual mirror level, present since device fabrication. We highlight the fact that these effects have no impact in a typical DMD display mode, but they have to be taken into consideration and calibrated for MOS application. These numbers are very low when compared to the total 2 millions mirrors operating in the device.

This test revealed no degradation of the device when three consecutive cycles in EUCLID conditions are applied. The cold temperature step stress test and the nominal cold temperature test have been fully described previously. [8]

4.2 Thermal cycling

Thermal cycling has been done on one DMD mounted on a DMD board, and conducted at INAF/IASF's facility in Bologna in Italy, and first five cycles as well as the optical characterizations have been performed at LAM's facility in Marseille in France. An Angelantoni ACS Challenger 250 Climatic chamber located in a class 100.000 clean room was used for the 562 thermal cycles conducted at INAF/IASF. Two sets of cycles (249 and 313 cycles) have been applied, with intermediate and final optical characterization. No anomaly was observed on the DMD by visual inspection with unaided eye after the thermal cycling was completed but some dirt was deposited on the DMD window during cycling. In particular no cracks, no flakes were observed. The results for the reference measurement at +20°C are presented in Fig. 6 first row in three graphs showing the number and the locations of affected mirrors with 1 blocked, 4 lossy, and 15 weak mirrors. The results for the measurement at -40°C after the first serial of 254 cycles are given in Fig. 6 second row with 1 blocked, 2 lossy, and 7 weak mirrors. The results for the third measurement at -40°C after the second serial of 313 cycles are shown in Fig. 6 third row with 0 blocked, 6 lossy, and 30 weak mirrors.

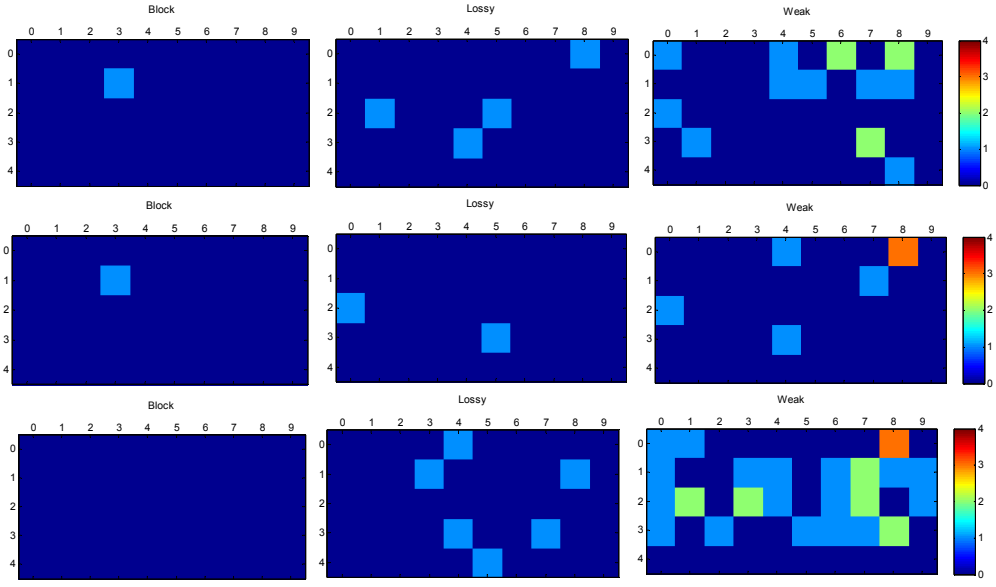

Fig. 6: First row: Location and numbers of affected mirrors at +20°C.
Second row: Location and numbers of affected mirrors at -40°C, after the first serial of 254 cycles.
Third row: Location and numbers of affected mirrors at -40°C, after completion of all cycles (567 cycles).

Either one or zero blocked mirror is observed during this test, located in zone 13. The measured throughput is at the limit between blocked and lossy mirror. Between two and six lossy mirrors have been observed during the thermal cycling test: for most of them, they are located in different places, these mirrors being at the limit between lossy and weak mirrors. The number of weak mirrors is in the same range before and after testing; a slight increase of this number could be due to the extra dirt on the window. From these charts, we clearly see that the same behavior is occurring for mirrors switching frequently (display mode in the central row) or in a static pattern during 1500s (EUCLID mission conditions), in the four other rows.

In conclusion of the thermal cycling, this test has been successfully completed. This shows that space conditions did not degrade the device performances, within this thermal cycling campaign.

4.3 Life test

The life test has been completed on one DMD device. The device was tested in EUCLID conditions, this means in vacuum, at -40°C and the device was operating with the following test cycle: pattern 1 is applied for 1500s (central pattern row is tilting in display mode while other pattern rows display a static pattern), the whole device is switching between pattern 1 and pattern 2 for 60s and pattern 2 is applied for 1500s (central pattern row is tilting in display mode while other pattern rows display a static pattern). By this way, there is an identical duty cycle for all mirrors. **The life test lasted for 1038 hours.** Full optical tests were done during the whole life test. Measurements were done at room temperature (reference measurement), a first test at cold temperature was done at T0, then 11 intermediate measurements were done, and finally, a last measurement was done at the end of the life test, after **1038h.**
During the whole test, the DMD operational temperatures were recorded:

- DMD heat sink temperature (close to the actual DMD component temperature point): **-41°C**
- DMD front mounting surface temperature: **-36°C**
- Thermal interface temperature: **-49°C**

We can note that when the DMD is turned off, a drop of **2-3°C** in temperature is revealed, showing the heating capability of the DMD chip due to its power consumption.
After recording all data, we used the analysis procedure described in paragraph 3 for extracting the number and the locations of affected mirrors (blocked, lossy, weak). The results for the reference measurement at +20°C are presented in Fig. 7 first row in three graphs showing the number and the locations of affected mirrors with 3 blocked, 7 lossy, 12 weak mirrors. The results for the last measurement at -40°C after 1038 hours of operation are shown in Fig. 7 second row with 3 blocked, 7 lossy, 8 weak mirrors. All intermediate tests are identical to these results with very little variation of only few mirrors for the weak case. From these charts, we clearly see that the same behavior is occurring for mirrors switching frequently (display mode in the central row) or in a static pattern during 1500s (EUCLID mission conditions), in the four other rows.

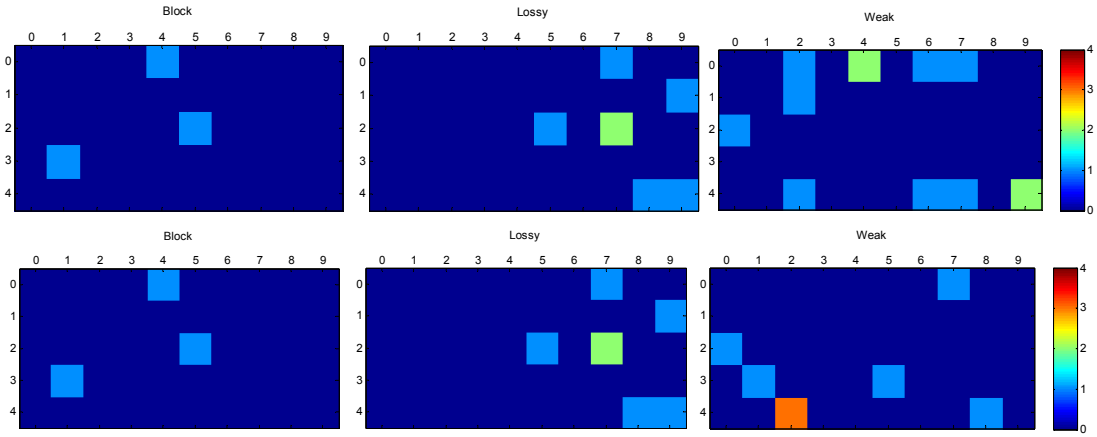

Fig. 7: First row: Location and numbers of affected mirrors at +20°C.
Second row: Location and numbers of affected mirrors at -40°C, after 1038 hours of life test.

In conclusion of the life test, this test has been successfully completed. Three blocked mirrors and five lossy mirrors have been observed, but they are detected at ambient, at cold temperature at the beginning of the test and at cold temperature at the end of the test; they are not a consequence of the space conditions applied to the device. Other

affected mirrors are only weak mirrors and their number is very low, with no increase while the life test is running. **This shows that space conditions did not degrade the device performances, within this life test period.**

5. RADIATION AND VIBRATIONS TESTING

Radiation and vibrations tests have been conducted on DMD devices. Results have been described extensively in previous papers. [8, 9] Total Ionizing Dose (TID) radiation tests established a tolerance level of 10 - 15 Krads for the DMD; at mission level, this limitation could likely be overcome by shielding the device. Vibration test conditions using the standards MIL-STD-883F, methods 2005 (vibration fatigue) and 2007 (vibration at variable frequency) condition A, and shock test condition B of the MIL-STD-883f Method 2002 were applied. It has been demonstrated that space conditions did not degrade device performances.

6. MICROMIRRORS THROUGHPUT ANALYSIS

From the recorded measurements, we have engaged a detailed micromirror throughput analysis. In paragraph 3, blocked, lossy and weak mirrors have been defined for mirrors exhibiting losses larger than 10%. In this paragraph, we consider micromirrors throughputs on the whole range. Calculation has been made on 12 experiments realized during the life test. The analysis is done on a typical zone, the zone # 25, considering 42177 micromirrors after removal of zone edges mirrors as well as mirrors affected by dust particles; the number of samples is large enough for having a good statistical analysis.

In order to define the accuracy of our measurements, we do standard deviation calculation for each set of measurements. These standard deviation values include:

- measurement precision
- throughput calculation method precision
- local mirror throughput variation

A typical histogram for a single experiment is shown in Fig. 8. The figure is very sharp with nearly all micromirrors included in the ±5% range. Note that we obtained a slight broadening of the histogram when the image is not perfectly focused, with marginal effect on the standard deviation value. We consider in this paragraph as "normal" any mirror having a throughput within this ±5% range during all experiments.

For all 12 considered experiments, the standard deviation is always smaller than 1.9%. Small and uniform standard deviation values show that our measurement set-up is very stable.

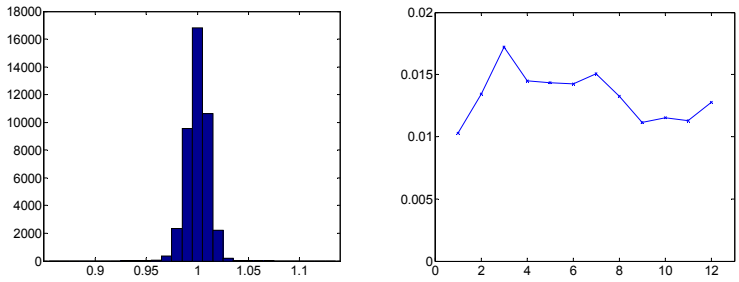

Fig. 8: Histogram for a single experiment and standard deviation calculated for all 12 experiments

When analyzing the evolution of each micro-mirror throughput, we have revealed four types of mirrors in zone 25:

- mirror always blocked
- weak mirror becoming "normal"
- mirrors with temporary throughput loss
- mirrors with temporary throughput increase

The throughput evolution for the first two cases have been detected only on one mirror for each type: one mirror is always blocked and one weak mirror is back to normal at the end of the life test (Fig. 9). All other mirrors show only temporary modification of their throughput. Some examples are given in Fig. 10: 2 mirrors show a throughput loss for the first measurements at cold temperature and then slowly back to normal for the following tests; 6 mirrors show a throughput loss for the first measurements at cold temperature and then stay at this value for the following tests; 2 mirrors show a throughput increase for the first measurements at cold temperature and then slowly back to normal for the following tests. Throughput loss and throughput increase are due to slight differences on the tilting angle and possible slight deformation of the mirror surface. Note that these variations are very limited, within the ±10% range.

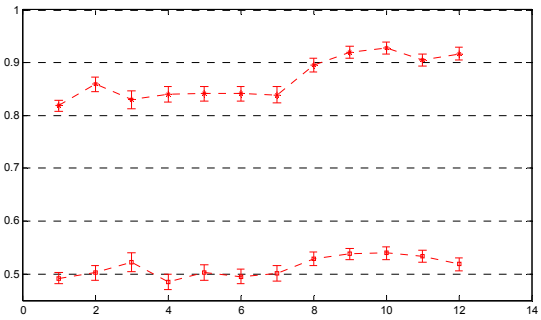

Fig. 9: Two mirrors throughput evolution during all 12 experiments; 1 blocked mirror and 1 weak mirror.

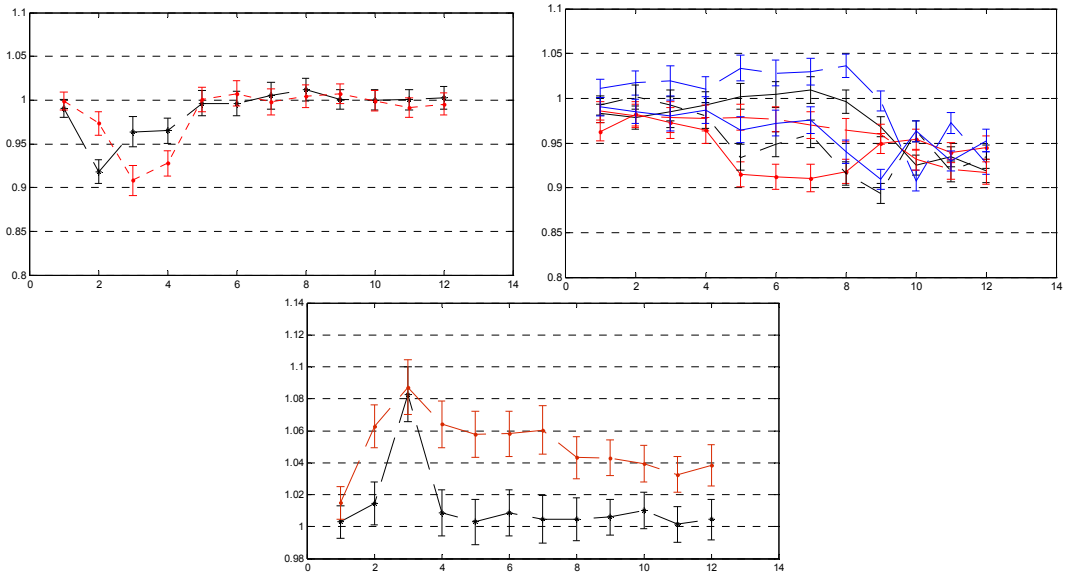

Fig. 10: Temporary degraded mirrors during all 12 experiments

We have gathered in the following tables the number of mirrors affected in the whole data set in absolute values for all measurements, when considering the relative evolution with respect to the first experiment at room temperature and with respect to the first experiment at cold temperature. Permanently and temporarily affected mirrors have been separated. Both throughput loss and throughput increase are considered and limits at 40%, 20%, 10 %, 8% and 5% are marked. In zone 25, for all measurements, only one mirror is always blocked and one mirror is considered temporary weak. Within the ±8% range, a very low number of additional temporary affected mirrors (around 20 mirrors with throughput loss and throughput increase) are in addition to the previous ones. In the ±5% range, the number of affected mirrors rises to 300 mirrors. However, in order to reveal the impact of testing DMDs in space environment, let's count the affected mirrors with respect to the initial room temperature measurement (Fig. 11): 4 mirrors on a total of 42177 mirrors exhibit a permanent throughput loss larger than 5% (but lower than 10%), no mirrors exhibit a permanent throughput increase larger than 5%, 86 mirrors exhibit a temporary throughput loss larger than 5%, and 88 mirrors exhibit a temporary throughput increase larger than 5%. All temporary variations do not exceed 10%.

		Number of mirrors with throughput loss				
		Blocked	-40%	-20%	-10%	-8%	-5%
All measurement sets	permanent	1	1	1	1	2
	temporary	0	0	1	10	164
With respect to +20°c	permanent	0	0	0	0	4
	temporary	0	0	1	4	86
With respect to -40°c	permanent	0	0	1	1	1
	temporary	0	0	0	3	31

		Number of mirrors with throughput increase				
		Extra-Brightness				
		40%	20%	10%	8%	5%
All measurement sets	permanent	0	0	0	0	1
	temporary	0	0	2	8	129
With respect to +20°c	permanent	0	0	0	0	0
	temporary	0	0	1	11	88
With respect to -40°c	permanent	0	0	0	0	0
	temporary	0	0	2	9	57

Then, during the life test in space conditions, we could evaluate the throughput evolution while being at cold temperature. We have counted the affected mirrors with respect to the first cold temperature measurement at -40°C (Fig. 12): 1 mirror on a total of 42177 mirrors exhibits a permanent throughput loss larger than 5% (but lower than 12%), no mirrors exhibit a permanent throughput increase larger than 5%, 31 mirrors exhibit a temporary throughput loss larger than 5%, and 57 mirrors exhibit a temporary throughput increase larger than 5%. All temporary variations do not exceed 10%. **The operation of the DMD during a long time in space environment did not generate any additional degradation compared to operation at room temperature.**

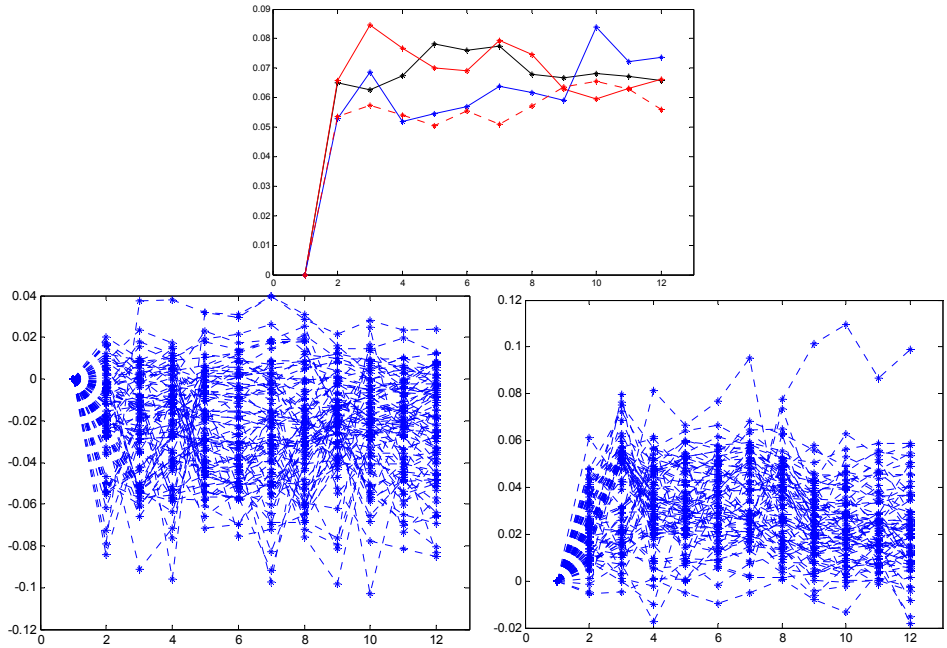

Fig. 11: Throughput with respect to room temperature meas.; 4 permanently affected mirrors and temporarily affected mirrors

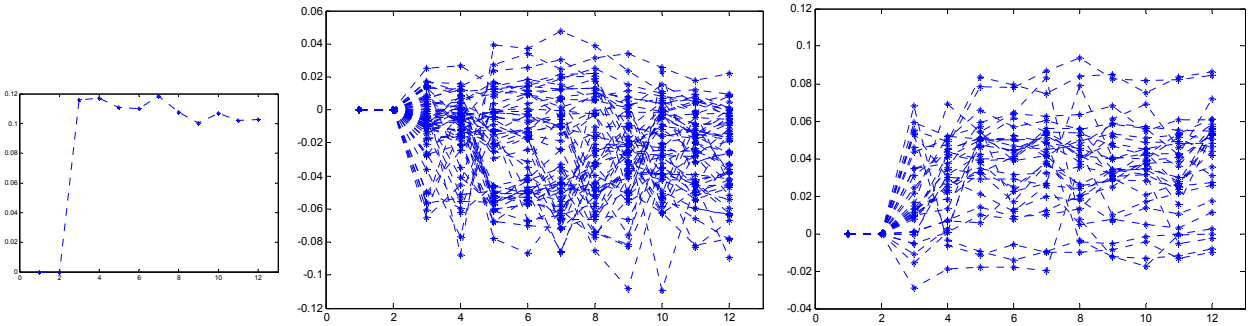

Fig. 12: Throughput with respect to first cold temperature measurement; permanent and temporarily affected mirrors

In Fig. 13 is presented the throughput of 1000 mirrors calculated for all 12 experiments. Throughput values stay nearly constant for all of them, in + / - 5% range. The throughputs of the only affected mirrors (blocked and weak mirrors) are also displayed.

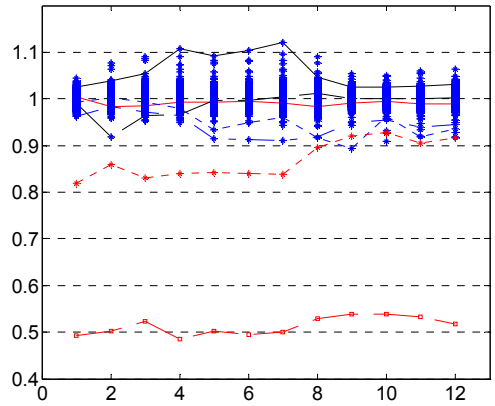

Fig. 13: Throughput of 1000 mirrors, (nearly all in + / - 5%) and one blocked and one weak mirrors

7. MOS-like TESTS

In order to evaluate the capability of a DMD device to select objects in a field of view, we have developed a dedicated test set-up, demonstrating the concept of a DMD-based MOS spectrograph. From a field of view simulator, objects could be selected with the DMD device. Then, device performances have been measured and object selection procedure has been evaluated.

For the MOS test, an optical characterization test setup has been developed at LAM. The bench is used as a photometric bench, and the FOV is imaged on a 1kx1k camera in order to get enough resolution on each micro-mirror. Each micro-mirror is imaged on about 9 x 9 detector pixels. In comparison with the set-up developed for vacuum and low temperature testing (4 x 4 detector pixels / micro-mirror), the optical magnification is higher in this new set-up; we want then to get a higher photometric accuracy in DMD performance parameters, as well as a higher spatial resolution on each micro-mirror. We set a 24° angle between input and output beam, and both input and output beam have been set to F/3. In front of the camera, we are able to introduce a neutral density filter in order to increase the dynamic range of the bench. This feature is very important for the precise DMD contrast determination. A FOV containing three objects was imaged on the DMD device surface (Fig. 14a). In Fig. 14b, the same FOV is presented, but the DMD is programmed for selecting the left-hand object (the mirrors are ON only on the object to be selected, and the rest of the mirrors are OFF). **This picture shows the full capability of the DMD device to generate any slit pattern (reflective slit) sending the light towards the spectrograph, when all other sources as well as background are hidden by the OFF micro-mirrors.** The contrast of a micro-mirror is defined as the ratio of the throughput when the mirror is in ON position with respect to the mirrors in OFF position. In order to be as accurate as possible, the throughput is integrated within a mask applied on a whole micro-mirror. The background light has been removed. **This gives a final value of the contrast of 2250.** Contrast has been measured on several mirrors and they exhibit identical values.

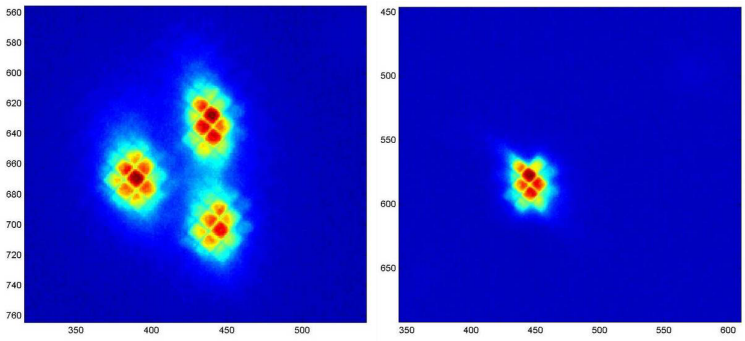

Fig. 14: (a) FOV with three objects imaged on the DMD device surface. (b) Same FOV when the DMD is programmed in order to select the left-hand side object (the mirrors are ON only on the object to be selected, and the rest of the mirrors are OFF).

8. CONCLUSION

Large field of view surveys with a high density of objects such as high-z galaxies or stars benefit of multi-object spectroscopy (MOS) technique. Digital Micromirror Devices (DMD) could act as objects selection reconfigurable mask. ESA has engaged with Visitech and LAM in a technical assessment of using a DMD from Texas Instruments (2048 x 1080 mirrors on a 13.68µm mirror pitch) for space applications. Specialized driving electronics and a cold temperature test set-up have been developed.

Our tests reveal that the DMD remains fully operational at -40°C and in vacuum. The 1038 hours life test in space survey conditions (-40°C and vacuum), has been successfully completed. The device was operating continuously with typical MOS patterns. The numbers of affected mirrors are very low compared to the 2 million mirrors of the DMD array. Total Ionizing Dose (TID) radiation tests established a tolerance level of 10 - 15 Krads for the DMD; at mission level, this limitation could likely be overcome by shielding the device. Thermal cycling (over 500 cycles between room temperature and cold temperature, on a non-operating device) and vibration and shock tests have also been done; no degradation is observed from the optical measurements. Detailed analysis of micromirror throughputs has also been studied for a whole set of tests, and shows a rather low variation and no impact of the space environment.

These results do not reveal any show-stopper concerning the ability of the DMD to meet environmental space requirements. Insertion of such devices into final flight hardware would still require additional efforts such as development of space compatible electronics, and original opto-mechanical design of the instrument.

From an ESA perspective, the micromirror arrays have therefore achieved a reasonable TRL (Technology Readiness Level). Insertion of such devices into final flight hardware would still require additional efforts (estimation is approximately 2 years) in terms of change of the window coating, re-development of space compatible electronics as well as a different package interface compatible with spacecraft launch conditions.

ACKNOWLEDGEMENT

The authors thank Jean-Antoine Benedetti, Philippe Laurent and Vincent Herault from LAM for their assistance during the tests. This work is partly funded by ESA, CNRS, Provence-Alpes-Cote d'Azur regional council and Conseil General des Bouches-du-Rhone county council.

REFERENCES

[1] R. Burg, P.Y. Bely, B. Woodruff, J. MacKenty, M. Stiavelli, S. Casertano, C. McCreight and A. Hoffman, "Yardstick integrated science instrument module concept for NGST", in *Proceedings of the SPIE conference on Space Telescope and Instruments V*, SPIE **3356**, 98-105, Kona, Hawaii, 1998

[2] F. Zamkotsian, K. Dohlen, D. Burgarella, V. Buat, "Aspects of MMA for MOS: optical modeling and surface characterization, spectrograph optical design", in *Proceedings of the NASA conference on "NGST Science and Technology Exposition"*, ASP Conf. Ser. **207**, 218-224, Hyannis, USA, 1999

[3] M. Robberto, A. Cimatti, A. Jacobsen, F. Zamkotsian, F. M. Zerbi, "Applications of DMDs for Astrophysical Research", in *Proceedings of the SPIE conference on MOEMS 2009*, Proc. SPIE **7210**, San Jose, USA (2009)

[4] M. J. Li; A. D. Brown; A. S. Kutyrev; H. S. Moseley; V. Mikula, " JWST microshutter array system and beyond", Proc. SPIE 7594, San Francisco, USA, 2010

[5] M. Canonica, S. Waldis, F. Zamkotsian, P. Lanzoni, W. Noell, N. de Rooij, " Development of MEMS-based programmable slit mask for multi-object spectroscopy ", in *Proceedings of the SPIE conference on Astronomical Telescopes and Instrumentation*, Proc. SPIE **7739**, San Diego, USA (2010)

[6] F. Zamkotsian, K. Dohlen, "Performance modeling of JWST Near Infrared Multi-Object Spectrograph," in *Proceedings of the SPIE conference on Astronomical Telescopes and Instrumentation 2004*, Proc. SPIE **5487**, Glasgow, United Kingdom (2004)

[7] F. Zamkotsian, J. Gautier, P. Lanzoni, "Characterization of MOEMS devices for the instrumentation of Next Generation Space Telescope," in *Proceedings of the SPIE conference on MOEMS 2003*, Proc. SPIE **4980**, San Jose, USA (2003)

[8] F. Zamkotsian, E. Grassi, P. Lanzoni, R. Barette, C. Fabron, K. Tangen, L. Marchand, L. Duvet "DMD chip space evaluation for ESA EUCLID mission," in *Proceedings of the SPIE conference on MOEMS 2010*, Proc. SPIE **7596**, San Francisco, USA (2010)

[9] F. Zamkotsian, P. Lanzoni, E. Grassi, R. Barette, C. Fabron, K. Tangen, L. Valenziano, L. Marchand, L. Duvet "Space evaluation of 2048 x 1080 mirrors DMD chip for ESA EUCLID mission," in *Proceedings of the SPIE conference on Astronomical Telescopes and Instrumentation*, Proc. SPIE **7731**, San Diego, USA (2010)

[10] F. Zamkotsian and K. Dohlen, "Surface characterization of micro-optical components by Foucault's knife-edge method: the case of a micro-mirror array", Applied Optics, **38** (31), 6532-6539 (1999)

[11] A. Liotard, F. Zamkotsian, "Static and dynamic micro-deformable mirror characterization by phase-shifting and time-averaged interferometry", in *Proceedings of the SPIE conference on Astronomical Telescopes and Instrumentation 2004*, Proc. SPIE **5494**, Glasgow, United Kingdom (2004)